Predicting the electrochemical behavior of Fe(II) complexes from ligand orbital energies

*Daniel C. Ashley and Elena Jakubikova**

Department of Chemistry, North Carolina State University, Raleigh, North Carolina 27695, United States

ABSTRACT: An attractive strategy for harvesting solar energy is to use dye-sensitized solar cells employing earth-abundant Fe(II) chromophores. These dyes need to meet several criteria to be effective for this purpose, including air stability, and an ability to be regenerated by common electrolytes. Both of these properties are related to the Fe(III/II) reduction potentials. Here we show how the Fe(III/II) reduction potentials of Fe(II) complexes can be estimated from a single experimental Fe(III/II) reduction potential and computationally cheap calculations on single isolated ligands. This method requires refinement, but could prove highly useful for large-scale computational screening and design of Fe(II) dyes.

Introduction

One of the problems facing mankind today is our rapidly diminishing energy resources. The most effective solution to this problem is the one already developed by nature: Harnessing the energy of light from the sun to perform useful work.[1] Traditional silicon based solar cells are effective, but they have complex manufacturing processes that are expensive in terms of both money and energy.[2] Dye-sensitized solar cells (DSSCs) are an alternative way to harvest solar energy, where a molecular chromophore (dye) becomes excited by a photon of light and transfers the resulting high energy electron to a TiO_2 semiconductor.[1-3] Eventually, the oxidized dye is regenerated by reduction via an electrolyte (typically I_3^-/I^-). There are many working parts in a DSSC that require careful tuning to be effective, and several of these concern the dye itself. An ideal dye will display high-intensity long-wavelength absorbance, long-lived excited state lifetimes, and efficient interfacial electron transfer to the semiconductor.[4,5] The dyes also need to be both air stable[6] and the oxidized dyes should have a reduction potential similar to that of the electron-transfer agent to minimize overpotential; the oxidized dye should readily accept an electron from the electrolyte source. Hence, being able to control and predict the redox potentials of dyes can greatly assist in the process of developing efficient DSSCs.

Transition metal complexes naturally make good dye candidates, as they have widely tunable absorbances, often in the visible range. Ruthenium dyes have found great success for this purpose, but it would be desirable to replace ruthenium with earth-abundant iron to lower the cost of making the DSSC.[7] Recently, we have explored the connection between the Fe(III) to Fe(II) reduction potential (E_{Fe}), spin-state energetics (important for excited state lifetime) and oxidative stability.[8] The combination of modern density functional theory (DFT) and implicit PCM solvation models has been shown in numerous instances to accurately predict the redox potentials of transition metal complexes.[8-10] While DFT is a highly affordable electronic structure method, it can still become computationally expensive for large systems, or for screening over a large set of complexes. It would be ideal if DFT could be used on a smaller fragment of the complex to make the same predictions, and below we detail the early successes and failures we have had in this regard.

In this work, we explore an approach to predicting redox potentials of Fe(II) complexes based on the properties of individual ligands by re-examining a series of substituted $[Fe(bpy)_3]^{2+}$ complexes, where E_{Fe} has already been calculated and/or measured. Our previous work showed that metal-ligand electrostatic interactions play a large role in dictating E_{Fe}.[8] These interactions correlate well with the donor strength of the ligand, which was estimated from the standard Hammett parameter (σ) for the functional group on the ligands. Ligands with more negative Hammett parameters (i.e. greater donor strength) induced greater destabilization of the metal t_{2g} orbitals, thereby making the Fe(II) complex easier to oxidize. It stands to reason then that if the metal is held constant (i.e. if it is always taken as divalent iron), the change in E_{Fe} can be estimated from the changes in donor strength of the ligand. From a practical standpoint, Hammett parameters could be used for screening potential Fe(II) complexes without time-consuming calculations or measurements, however, such a method is limited by the availability of experimentally measured Hammett parameters. Standard molecular orbital theory suggests that the orbitals on the isolated ligand should be higher in energy (more basic; more donating) if the ligand itself is functionalized with a less electronegative substituent. It follows then that calculated ligand orbital energies could be used to predict the redox properties of their corresponding Fe(II) complexes.

The goal in this work is to use selected molecular orbitals (ϕ) of isolated ligands from the Fe(II) complexes (in this case they are all substituted bpys, where bpy = 2,2′-bipyridine) and compare how much the energies of these molecular orbitals (ε) shift relative to the

molecular orbital energies of the reference ligand (the corresponding molecular orbital and its energy in the reference complex are referred to as ϕ_{ref} and ε_{ref}, respectively). This reference ligand is selected to belong to a complex with a known value of E_{Fe}, in this case the unsubstituted $[Fe(bpy)_3]^{2+}$ complex, and the magnitude of the shift in orbital energy is taken as the estimate of the magnitude of shift in E_{Fe} ($E_{est} - E_{ref}$) as shown in Equation 1:

$$E_{est} = E_{ref} - (\epsilon - \epsilon_{ref}) \qquad (1)$$

Here this idea was tested utilizing different methods of structure optimization, solvent models, and choice of ϕ to evaluate if it holds promise for large-scale screening of transition metal complexes for their use in DSSCs or other applications.

Computational methods

All DFT calculations were performed with the BP86[11-13] functional. The 6-311+G** basis set was utilized on all atoms,[14-17] with the exception of iodine, where the SDD basis sets and accompanying pseudopotentials were used.[18] The ligand structures were either taken directly from an optimized metal complex (**complex**) and used as is, or they were optimized by starting from that geometry (**relaxed**). Calculations were performed either in the gas phase or incorporating solvation through the IEF-PCM implicit solvation model (acetonitrile, $\varepsilon = 37.5$). An ultrafine integral grid was employed for all calculations. Frequencies were calculated for all optimized structures using the harmonic oscillator approximation to verify that the structures were true minima with no imaginary frequencies. Wavefunctions for all calculations were ensured to be minima through stability analysis. All DFT calculations were performed with the Gaussian 09 software package Revision D.01.[19]

Results and Discussion

Twenty-one substituted $[Fe(bpy)_3]^{2+}$ complexes were considered and are shown in Figure 1. All values of E_{Fe} were calculated with DFT and are taken directly from Ref. 8. The unsubstituted complex (Y=H) was used as the reference compound, and E_{ref} was set to the experimentally determined value of E_{Fe}, 1.27 V vs. NHE.[8,20] The structure of the ligand could be taken directly from the optimized coordinates of the iron complex (**complex**) or those coordinates could be used as the starting point for a geometry optimization (**relaxed**). Note that these optimized structures correspond to the local rather than global minima, as the bipyridine molecules were always in a *cis* conformation with the nitrogen atoms pointing in the same direction (see Figure 2a). This was done intentionally so as to maximize the similarity between the **relaxed** and **complex** structures without imposing any artificial constraints. The global minimum for a substituted bipyridine corresponds to the *trans* conformation, with the energy difference between the *cis* (**relaxed**) and *trans* conformations being calculated as ~5-8 kcal/mol throughout the series. Additionally, a choice needed to be made as to whether or not solvent should be modeled in the calculation, given that accurate calculation of reduction potentials requires inclusion of solvation effects. As such, both solvated single points on gas-phase optimized structures and optimizations performed with the solvent model were also performed.

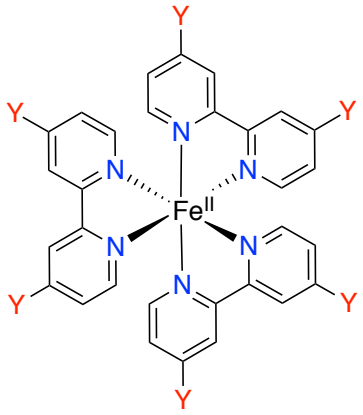

Y = NEt_2, NMe_2, NH_2, OH, OMe, Me, SH, F, SMe, H, CH_2SCN, Cl, Br, I, CO_2H, SOMe, CF_3, CN, SO_2Me, NO_2, SO_2Cl

Figure 1. Substituted $[Fe(bpy)_3]^{2+}$ series considered in this study.

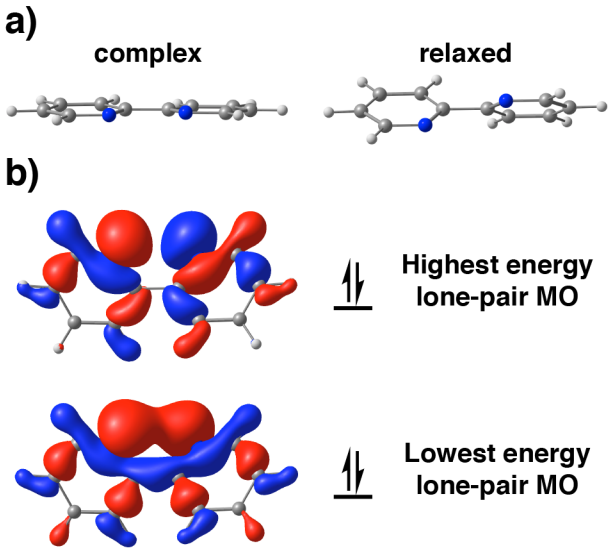

Figure 2. a) Examples of the **complex** and **relaxed** structures for unsubstituted bpy. b) The two relevant lone pair (LP) orbitals (isovalue = 0.03 e/Å^3) of **relaxed**, unsubstituted bpy.

Equation 1 also requires choosing what molecular orbital will be taken as ϕ. Three different choices of ϕ were made in this study. The simplest (advantageous

for screening over large datasets) is to simply take the HOMO from each ligand as ϕ. The HOMO has a distinct physical meaning in DFT, as it is the negative ionization potential of the complex.[21] The other choices of ϕ necessitated examining the ligand orbitals themselves, specifically to locate the molecular orbitals that corresponded with the in-phase and out-of-phase combinations of nitrogen-lone pairs (LPs) from each pyridine ring (see Figure 2b). The second option for choosing ϕ is to use the out-of-phase LPs, as this pertains to picking the highest energy orbitals that are also relevant for electrostatically perturbing the metal-based orbitals. Note that often, but not always, the highest energy LP was also the HOMO. The final option explored was to average the energy of the two LP orbitals.

Table 1. Mean signed error (MSE) and the standard deviation of the error (SDE) for E_{est} using different structures, solvation models and choices of ϕ. Also listed are the correlation coefficients (R^2) determined from the relationship of E_{est} with E_{Fe}.

Structure	*Solvation*	*Choice of ϕ*	*MSE (eV)*	*SDE (eV)*	R^2
Complex	Gas	HOMO	0.14	0.15	0.96
		Highest LP	0.14	0.15	0.96
		Average LP	0.15	0.16	0.95
	Solvent	HOMO	-0.02	0.31	0.91
		Highest LP	0.01	0.35	0.94
		Average LP	0.03	0.37	0.92
Relaxed	Gas	HOMO	0.12	0.21	0.89
		Highest LP	0.19	0.20	0.95
		Average LP	0.19	0.19	0.95
	Solvent	HOMO	-0.11	0.31	0.78
		Highest LP	0.05	0.40	0.92
		Average LP	0.05	0.40	0.91

Table 1 collects the mean signed error (MSE) and the standard deviation of the error (SDE) for each combination of methodology choices. Here error is defined as $E_{est} - E_{Fe}$, always using the calculated value of E_{Fe}. The MSE reflects how accurate the method is overall at predicting E_{Fe}, while SDE informs on how reliable and consistent the error is. Several observations can be made from this data. Regardless of the choice of ϕ, the effect of relaxing the geometry is always to modestly increase SDE (by ~0.05 eV) and usually increase MSE (the largest increase is by ~0.09 eV but in most cases, this is closer to ~0.05 eV). This shows that optimizing the geometry has a deleterious effect on the prediction of E_{Fe}, an expected result as the **relaxed** ligands are not replicating their environment in the metal complex as accurately. The decrease in accuracy and reliability is not so large as to absolutely necessitate using the **complex** geometries, however, which is ideal considering there can be instances where it would be desirable to predict E_{Fe} for a complex where the structure is not known experimentally or computationally. Conversely, an alternative usage of this methodology that exploits the higher accuracy of the **complex** geometries would be to use ligand structures from crystal structure data for given metal complexes. This would only require some minimal geometry clean-up (using cheap force-field based methods for example) before performing a DFT single point energy calculations, and would hence maximize efficiency and accuracy.

The effect of solvation is less straightforward. Solvation tends to decrease the MSE, but this may not be a reflection of higher accuracy, but rather that the error is less systematic, and the overestimation of some values is cancelled out by the underestimation of others. Evidence for this is that the SDE always increases upon inclusion of solvation, sometimes so much as doubling in the process. Overall this large drop in predictability suggests that E_{est} is best determined in the gas phase. Note that the ligands in this study are neutral, and that it is possible that inclusion of solvent will be more beneficial for charged ligands. The last factor is choice of ϕ. In the gas phase this has no effect on SDE, but for **relaxed** geometries the choice of HOMO results in a smaller MSE by 0.07 eV. It is unclear if this is a meaningful result given that there are only a few complexes where the HOMO is not the highest energy LP (see Table S1 for full list of relevant orbital energies). This may be a fortuitous cancellation of error, or it may reflect that the HOMO energy is the best indicator of the ligand's donor strength, regardless of whether or not the types of orbitals being compared are consistently chosen. It is probably most prudent to specifically choose the highest LP as ϕ until this analysis can be repeated with a larger test set.

Figure 3 shows the correlation between E_{est} and E_{Fe} for the gas phase **relaxed** geometries using the highest LP as ϕ (other methodologies and orbital choices are shown in Figures S1-S6). If the method was perfect the slope would be equal to one, the intercept would be zero, and R^2 would be one. While the slope and intercept can be used to gauge accuracy and precision as well as the MSE and SDE, R^2 is particularly useful, as it gives a

measure of correlation, and a gauge of how good E_{est} is at predicting the trends in E_{Fe}. Note that R^2 is larger than 0.80 for all cases but one, and in most cases, is above 0.90 (See Table 1), demonstrating that although this general method still has considerable errors in predicting absolute values of E_{Fe}, it seems to be highly useful for predicting trends in E_{Fe}. Note that using the highest LP of the gas phase **complex** geometries predicts trends in E_{Fe} (R^2 = 0.96) equally well as using the highest LP of the gas phase **relaxed** geometries (R^2 = 0.95) despite the former having smaller MSE and SDE.

Figure 3 also shows where using orbital energy shifts is most effective and where it breaks down. The agreement between E_{est} and E_{Fe} is best for complexes with significantly positive E_{Fe} (greater than 1.5 V vs. NHE). As the reduction potentials become more negative this error progressively increases, with the trend lines for each data set increasingly deviating from the perfect fit. In fact, the improved performance of the **complex** geometries arises from these geometries being more accurate for complexes with more negative reduction potentials. From a practical standpoint, this data shows that the orbital energy shift method of estimating E_{Fe} will be more reliable for more electron-deficient, strongly oxidizing complexes. Note that the relationship between the **complex** and **relaxed** geometries is not universal for all methodologies, and is significantly different in some cases (Figure S4). Finally, when considering calculations employing solvent. Figures S4-S6 confirm that the low MSE discussed above is not a reflection of high accuracy, but rather a cancellation of errors between complexes that significantly overestimate and significantly underestimate E_{Fe}.

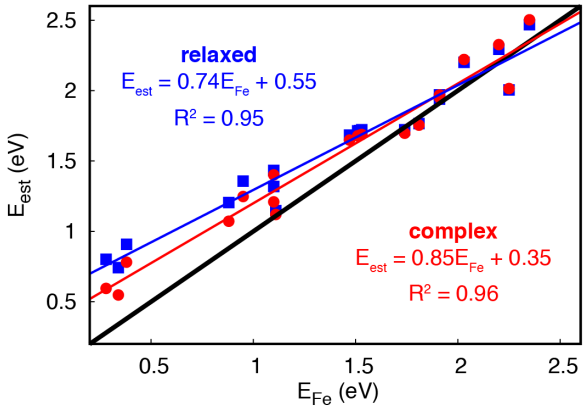

Figure 3. Correlation of E_{est} with E_{Fe} for the **relaxed** (blue squares) and **complex** (red circles) geometries determined in the gas phase using the highest LP as ϕ. The thick black line represents a perfect fit. All potentials are given in eV vs. NHE.

The data presented thus far has been for compounds that are highly similar to the reference compound, unsubstituted $[Fe(bpy)_3]^{2+}$. To see how successful the proposed methodology is for Fe(II) complexes with more diverse ligand environments, E_{est} was calculated for seven different homoleptic Fe(II) complexes where E_{Fe} and the crystal structure are experimentally known.[22-29] The results of these calculations are presented in Table 2 and the ligands used are shown in Figure 4. The only data used to determine E_{est} for this set of complexes was the experimental E_{ref} and calculated ε_{ref} for $[Fe(bpy)_3]^{2+}$, and the calculated ε for the ligand in question. The **complex** geometries for the ligands were taken directly from the crystal structures of the Fe(II) complexes themselves, after allowing all of the hydrogen atoms to optimize (due to the low accuracy of hydrogen atom placement in the crystal structures). Full optimization of the **complex** geometry generated the **relaxed** geometry, as before. Based on the previous results, the analysis was only conducted in the gas phase, using the highest LP as ϕ.

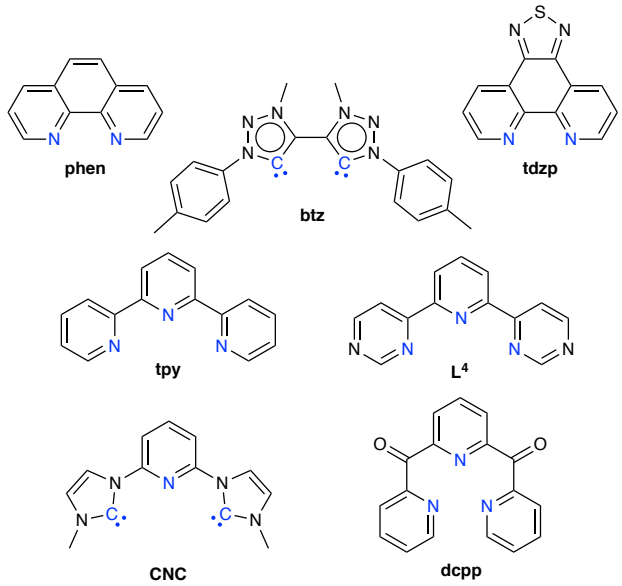

Figure 4. Structures and abbreviations of additional ligands considered.

Table 2. Reported are the experimental values of E_{Fe} for the given complexes and the error when calculated with the given geometries (error is still defined as $E_{est} - E_{Fe}$). All values are calculated in the gas phase using the highest LP as ϕ. All potentials are reported vs. NHE and all values are given in eV.

Compound	E_{Fe}	*error* ***complex***	*error* ***relaxed***	*error* ***trans***
$[Fe(phen)_3]^{2+}$	1.41	-0.03	-0.32	--
$[Fe(tdzp)_3]^{2+}$	1.19	0.45	0.17	--
$[Fe(btz)_3]^{2+}$	0.07	-0.89	--	0.17
$[Fe(tpy)_2]^{2+}$	1.36	-0.62	-0.16	-0.10
$[Fe(L^4)_2]^{2+}$	1.63	-0.36	-0.20	-0.08
$[Fe(CNC)_2]^{2+}$	0.96	-1.26	-0.78	-0.49
$[Fe(dcpp)_2]^{2+}$	1.94	-0.94	-0.89	-0.62

While the **complex** geometries gave superior results for the substituted $[Fe(bpy)_3]^{2+}$ series (when the highest LP was chosen as ϕ the MSE and SDE were ~0.05 eV smaller), for the test set they only gave good results for $[Fe(phen)_3]^{2+}$ where the error was only -0.03 eV, likely because of the strong resemblance between phen and bpy. All other values of E_{est} were in error by amounts ranging from 0.45 to 1.26 eV. The reason for this is likely that even though the **complex** geometries are better reflections of the actual ligand environment in the metal complex, for ligands that are drastically different from bpy they do not benefit from the error cancellation of comparing one strained substituted bpy ligand to another. Using the **relaxed** geometries produced substantial improvements in the calculated values of E_{Fe} (values of E_{est} were now only in error by amounts ranging from 0.16 to 0.89 eV) for every complex except $[Fe(phen)_3]^{2+}$, again due to phen's similarity to bpy.

Optimization of the highly strained btz ligand automatically converged to the ***trans*** orientation described earlier, which prompted consideration of the ***trans*** arrangement of donor atoms for the other ligands when possible (the fused ring structure of phen and tdzp prevents this). Note that using the ***trans*** geometry on the substituted $[Fe(bpy)_3]^{2+}$ series gave almost identical MSE, SDE, and R^2 to the gas phase **relaxed** geometries using the highest LP as ϕ (0.22 eV, 0.20 eV, and 0.93 respectively). For the remaining compounds of the test set, however, it gave further improved results (values of E_{est} were now only in error by amounts ranging from 0.08 to 0.62 eV). Overall, this shows that **complex** geometries should be used for calculating E_{est} if the compound in question is highly similar to the reference molecule; otherwise partially (**relaxed**) or fully (***trans***) optimized ligands will be more successful. It is encouraging to see that the method is able to perform well for the diverse ligands tested, with errors below 0.2 V often being achieved, but some ligands are still too different from bpy to yield accurate results. While using the ***trans*** geometries does significantly improve the accuracy of E_{est}, E_{est} was still off by ~0.5 V for $[Fe(CNC)_2]^{2+}$ and $[Fe(dcpp)_2]^{2+}$.

Conclusions

DFT calculations on isolated ligands can be used to estimate the changes in Fe(III/II) reduction potentials of Fe(II) bipyridine complexes. This is accomplished by assuming that the energy shifts of the HOMO and/or σ-donor orbitals on the isolated ligands correspond to the shifts in reduction potentials of the corresponding metal complexes. This follows because the orbital energy shifts of the ligand are related to the donor-strength of the ligand, which heavily dictates metal-ligand electrostatic interactions. Using the ligand structures exactly as they are in the optimized metal complex is ideal, but optimized ligands also perform reasonably well. In general solvation corrections make the predictions erratic, and better results are obtained in the gas-phase, although this may not be true for charged ligands. Using $[Fe(bpy)_3]^{2+}$ as a reference compound, reasonably accurate (errors amounting to no more than 0.2 eV) predictions of Fe(III/II) reduction potentials could be made when using several other different ligand types, but there were some instances where the ligand was too different from bpy for the errors to be less than ~0.5 eV. While the estimations of reduction potentials from this methodology are generally not quantitative, they perform well for predicting qualitative trends in chemical behavior, and as such they could be useful for large-scale screening of ligands for tuning metal complex reduction potentials. Overall, the results presented here show potential for predicting the redox behavior of Fe(II) complexes, which can aid in designing transition metal dyes with appropriate criteria to function in DSSCs or other photochemical devices.

ASSOCIATED CONTENT

Supporting Information

The Supporting Information is available free of charge online. Provided are additional plots of the correlation between E_{est} and E_{Fe}, all of the calculated orbital energies, all of the values of E_{est}, and xyz coordinates of all complexes considered (PDF).

AUTHOR INFORMATION

Corresponding Author

* ejakubi@ncsu.edu

ORCID

Daniel C. Ashley: 0000-0002-8838-4269

Elena Jakubikova: 0000-0001-7124-8300

ACKNOWLEDGMENT

We gratefully acknowledge support from the National Science Foundation (grant CH-1554855). We also acknowledge the use of the computing resources of the High-Performance Computing Center at NCSU.

REFERENCES

(1) Ardo, S.; Meyer, G. J., Photodriven Heterogeneous Charge Transfer with Transition-Metal Compounds Anchored to TiO_2 Semiconductor Surfaces. *Chem. Soc. Rev.* **2009**, *38*, 115-164.

(2) Grätzel, M., Solar Energy Conversion by Dye-Sensitized Photovoltaic Cells. *Inorg. Chem.* **2005**, *44*, 6841-6851.

(3) O'Regan, B.; Gratzel, M., A Low-Cost, High-Efficiency Solar Cell Based on Dye-Sensitized Colloidal TiO_2 Films. *Nature* **1991**, *353*, 737-740.

(4) Mukherjee, S.; Torres, D. E.; Jakubikova, E., HOMO Inversion as a Strategy for Improving the Light-Absorption Properties of Fe(II) Chromophores. *Chem. Sci.* **2017**, *8*, 8115-8126.

(5) Jakubikova, E.; Bowman, D. N., Fe(II)-Polypyridines as Chromophores in Dye-Sensitized Solar Cells: A Computational Perspective. *Acc. Chem. Res.* **2015**, *48*, 1441-1449.

(6) Estrada-Montaño Aldo, S.; Ryabov Alexander, D.; Gries, A.; Gaiddon, C.; Le Lagadec, R., Iron(III) Pincer Complexes as a Strategy for Anticancer Studies. *Eur. J. Inorg. Chem.* **2017**, *2017*, 1673-1678.

(7) Ashley, D. C.; Jakubikova, E., Ironing out the Photochemical and Spin-Crossover Behavior of Fe(II) Coordination Compounds with Computational Chemistry. *Coord. Chem. Rev.* **2017**, *337*, 97-111.

(8) Ashley, D. C.; Jakubikova, E., Tuning the Redox Potentials and Ligand Field Strength of Fe(II) Polypyridines: The Dual π-Donor and π-Acceptor Character of Bipyridine. *Inorg. Chem.* **2018**, *57*, 9907-9917.

(9) Roy, L. E.; Jakubikova, E.; Guthrie, M. G.; Batista, E. R., Calculation of One-Electron Redox Potentials Revisited. Is It Possible to Calculate Accurate Potentials with Density Functional Methods? *J. Phys. Chem. A* **2009**, *113*, 6745-6750.

(10) Baik, M.-H.; Friesner, R. A., Computing Redox Potentials in Solution: Density Functional Theory as a Tool for Rational Design of Redox Agents. *J. Phys. Chem. A* **2002**, *106*, 7407-7412.

(11) Becke, A. D., Density-Functional Exchange-Energy Approximation with Correct Asymptotic Behavior. *Phys. Rev. A* **1988**, *38*, 3098-3100.

(12) Perdew, J. P., Density-Functional Approximation for the Correlation Energy of the Inhomogeneous Electron Gas. *Phys. Rev. B* **1986**, *33*, 8822-8824.

(13) Perdew, J. P., Erratum: Density-Functional Approximation for the Correlation Energy of the Inhomogeneous Electron Gas. *Phys. Rev. B* **1986**, *34*, 7406-7406.

(14) Krishnan, R.; Binkley, J. S.; Seeger, R.; Pople, J. A., Self-Consistent Molecular Orbital Methods. XX. A Basis Set for Correlated Wave Functions. *J. Chem. Phys.* **1980**, *72*, 650-654.

(15) McLean, A. D.; Chandler, G. S., Contracted Gaussian Basis Sets for Molecular Calculations. I. Second Row Atoms, Z=11–18. *J. Chem. Phys.* **1980**, *72*, 5639-5648.

(16) Clark, T.; Chandrasekhar, J.; Spitznagel, G. W.; Schleyer, P. V. R., Efficient Diffuse Function-Augmented Basis Sets for Anion Calculations. III. The 3-21+G Basis Set for First-Row Elements, Li–F. *J. Comp. Chem.* **1983**, *4*, 294-301.

(17) Frisch, M. J.; Pople, J. A.; Binkley, J. S., Self-Consistent Molecular Orbital Methods 25. Supplementary Functions for Gaussian Basis Sets. *J. Chem. Phys.* **1984**, *80*, 3265-3269.

(18) Bergner, A.; Dolg, M.; Küchle, W.; Stoll, H.; Preuß, H., Ab Initio Energy-Adjusted Pseudopotentials for Elements of Groups 13–17. *Mol. Phys.* **1993**, *80*, 1431-1441.

(19) Frisch, M. J.; Trucks, G. W.; Schlegel, H. B.; Scuseria, G. E.; Robb, M. A.; Cheeseman, J. R.; Scalmani, G.; Barone, V.; Mennucci, B.; Petersson, G. A.; Nakatsuji, H.; Caricato, M.; Li, X.; Hratchian, H. P.; Izmaylov, A. F.; Bloino, J.; Zheng, G.; Sonnenberg, J. L.; Hada, M.; Ehara, M.; Toyota, K.; Fukuda, R.; Hasegawa, J.; Ishida, M.; Nakajima, T.; Honda, Y.; Kitao, O.; Nakai, H.; Vreven, T.; Montgomery, J. A., Jr.; Peralta, J. E.; Ogliaro, F.; Bearpark, M.; Heyd, J. J.; Brothers, E.; Kudin, K. N.; Staroverov, V. N.; Kobayashi, R.; Normand, J.; Raghavachari, K.; Rendell, A.; Burant, J. C.; Iyengar, S. S.; Tomasi, J.; Cossi, M.; Rega, N.; Millam, N. J.; Klene, M.; Knox, J. E.; Cross, J. B.; Bakken, V.; Adamo, C.; Jaramillo, J.; Gomperts, R.; Stratmann, R. E.; Yazyev, O.; Austin, A. J.; Cammi, R.; Pomelli, C.; Ochterski, J. W.; Martin, R. L.; Morokuma, K.; Zakrzewski, V. G.; Voth, G. A.; Salvador, P.; Dannenberg, J. J.; Dapprich, S.; Daniels, A. D.; Farkas, Ö.; Foresman, J. B.; Ortiz, J. V.; Cioslowski, J.; Fox, D. J.; Gaussian, Inc.: Willingford CT, 2009.

(20) Lever, A. B. P., Electrochemical Parametrization of Metal Complex Redox Potentials, Using the Ruthenium(III)/Ruthenium(II) Couple to Generate a Ligand Electrochemical Series. *Inorg. Chem.* **1990**, *29*, 1271-1285.

(21) Kohn, W.; Becke, A. D.; Parr, R. G., Density Functional Theory of Electronic Structure. *J. Phys. Chem.* **1996**, *100*, 12974-12980.

(22) Lever, A. B. P. *Inorg. Chem.* **1990**, *29*, 1271-1285.

(23) Hoshina, G.; Ohba, S.; Tsuchiya, N.; Isobe, T.; Senna, M. *Acta Cryst.* **2000**, *C56*, e191-e192.

(24) de Souza, B.; Xavier, F. R.; Peralta, R. A.; Bortoluzzi, A. J.; Conte, G.; Gallardo, H.; Fischer, F. L.; Bussi, G.; Terenzi, H.; Neves, A. *Chem. Commun.* **2010**, *46*, 3375-3377.

(25) Chábera, P.; Kjaer, K. S.; Prakash, O.; Honarfar A.; Liu, Y.; Fredin, L. A.; Harlang, T. C. B.; Lidin, S.; Uhlig, J.; Sundström, V.; Lomoth, R.; Persson, P.; Wärnmark, K. *J. Phys. Chem. Lett.* **2018**, *9*, 459-463.

(26) Jamula, L. L.; Brown, A. M.; Guo, D.; McCusker, J. K. *Inorg. Chem.* **2014**, *53*, 15-17.

(27) Oshio, H.; Spiering, H.; Ksenofontov, V.; Renz, F.; Gütlich, P. *Inorg. Chem.* **2001**, *40*, 1143-1150.

(28) Cook, L. J. K.; Tuna, F.; Halcrow, M. A. *Dalton Trans.* **2013**, *42*, 2254-2265.

(29) Liu, Y.; Harlang, T.; Canton, S. E.; Chábera, P.; Suárez-Alcántara, K.; Fleckhaus, A.; Vithanage, D. A.; Göransson, E.; Corani, A.; Lomoth, R.; Sundström, V.; Wärnmark, K. *Chem. Commun.* **2013**, *49*, 6412.